Light-dependent K^+ Channels in the Mollusc *Onchidium* Simple Photoreceptors Are Opened by cGMP

Tsukasa Gotow[1] and Takako Nishi[2,3]

[1]Department of Physiology, Faculty of Medicine, Kagoshima University, Kagoshima 890-8520, Japan
[2]Laboratoire de Neurobiologie Cellulaire et Moleculaire, CNRS, 91198 Grif-sur-Yvette, Cedex, France
[3]Laboratory of Physiology, Senshu University, Kawasaki 214-8580, Japan

ABSTRACT Light-dependent K^+ channels underlying a hyperpolarizing response of one extraocular (simple) photoreceptor, Ip-2 cell, in the marine mollusc *Onchidium* ganglion were examined using cell-attached and inside-out patch-clamp techniques. A previous report (Gotow, T., T. Nishi, and H. Kijima. 1994. *Brain Res.* 662:268–272) showed that a depolarizing response of the other simple photoreceptor, A-P-1 cell, results from closing of the light-dependent K^+ channels that are activated by cGMP. In the cell-attached patch recordings of Ip-2 cells, external artificial seawater (ASW) was replaced with a modified ASW containing 150 mM K^+ and 200 mM Mg^{2+} to suppress any synaptic input and to maintain the membrane potential constant. When Ip-2 cells were equilibrated with this modified ASW, the internal K^+ concentration was estimated to be 260 mM. Light-dependent single-channels in the cell-attached patch on these cells were opened by light but scarcely by voltage. After confirming the light-dependent channel activity in the cell-attached patches, an application of cGMP to the excised inside-out patches newly activated a channel that disappeared on removal of cGMP. Open and closed time distributions of this cGMP-activated channel could be described by the sum of two exponents with time constants τ_{o1}, τ_{o2} and τ_{c1}, τ_{c2}, respectively, similar to those of the light-dependent channel. In both the channels, τ_{o1} and τ_{o2} in ms ranges were similar to each other, although τ_{c2} over tens of millisecond ranges was different. τ_{o1}, τ_{o2}, and the mean open time τ_o were both independent of light intensity, cGMP concentration, and voltage. In both channels, the open probability increased as the membrane was depolarized, without changing any of τ_{o2} or τ_o. In both, the reversal potentials using 200- and 450-mM K^+-filled pipettes were close to the K^+ equilibrium potentials, suggesting that both the channels are primarily K^+ selective. Both the mean values of the channel conductance were estimated to be the same at 62 and 91 pS in 200- and 450-mM K^+ pipettes at nearly 0 mV, respectively. Combining these findings with those in the above former report, it is concluded that cGMP is a second messenger which opens the light-dependent K^+ channel of Ip-2 to cause hyperpolarization, and that the channel is the same as that of A-P-1 closed by light.

KEY WORDS: primitive vision • cGMP-gated K^+ channels • phototransduction in vertebrates and invertebrates • guanylate cyclase activated by light

INTRODUCTION

The primary function of photoreceptor cells is to convert the light stimulus into an electrical signal, i.e., the receptor potential. Vertebrate photoreceptor cells are known to respond to light with a hyperpolarizing receptor potential, caused by the closing of cation channels that are open in darkness (for review see Yau and Baylor, 1989). In these photoreceptors, it has been established that cGMP acts as a final internal messenger which opens or activates the cation channels, allowing their cGMP-activated channels to close when light reduces the internal cGMP levels (Fesenko et al., 1985; Matthews and Watanabe, 1987). Only one known exception has been found in that extraocular photoreceptors of the lizard parietal eye respond to light with a depolarization instead, resulting from the opening of cation channels by the same cGMP as in the above hyperpolarizing photoreceptors (Solessio and Engbretson, 1993; Finn et al., 1997).

On the other hand, in the ocular photoreceptors studied to date on invertebrates that occupy most parts of the animal kingdom, a depolarizing or a hyperpolarizing receptor potential is mediated by opening the membrane cation channels in all cases (Bacigalupo and Lisman, 1983; Nagy and Stieve, 1990; Nasi and Gomez, 1992; Gomez and Nasi, 1994). However, we have found that both depolarizing and hyperpolarizing responses to light are caused by either opening or closing of the membrane K^+ channels in extraocular photoreceptor cells, the photoresponsive neurons within the same abdominal ganglion of the mollusc *Onchidium* (Gotow, 1989; Gotow et al., 1994; Nishi and Gotow,

Address correspondence to T. Gotow, Department of Physiology, Faculty of Medicine, Kagoshima University, 8-35-1 Sakuragaoka, Kagoshima 890-8520, Japan. Fax: 81-99-275-5470; E-mail: tsukasa@m.kufm.kagoshima-u.ac.jp

1998). These extraocular photoreceptors, designated as A-P-1, Es-1, Ip-2, and Ip-1 will be referred to as simple photoreceptor cells, in view of their lack of microvilli or cilia characteristic of most ocular photoreceptors (Nishi and Gotow, 1998). Thus, the simple photoreceptor, A-P-1 or Es-1, depolarized by light seems to be parallel to the vertebrate ocular photoreceptors in a sense that both of their light-dependent cation channels are closed by light, although the polarity of the receptor potential is the opposite. As expected from this parallelism, we have found that cGMP is also a second messenger activating the light-dependent K^+ channels in A-P-1 or Es-1, as in the light-dependent cation channels of the vertebrate photoreceptors described above (Nishi and Gotow, 1989; Gotow and Nishi, 1991; Gotow et al., 1994). Similarly, another type of simple photoreceptor, Ip-2 or Ip-1, hyperpolarized by light, could be regarded as a primitive model of most ocular invertebrate photoreceptors, because light opens the underlying cation channels (Nishi and Gotow, 1998).

However, the second messenger that is responsible for the mechanism causing these channels to open has not yet been definitely established. One major reason for the uncertainty about second messengers involved in invertebrate photoreceptors may be that the intact cell in cell-attached recordings studied so far is never voltage clamped.

In the present study, the membrane voltage of the intact cell, Ip-2 or Ip-1, was substantially held constant to permit the characterization of single channels in a cell-attached patch, using an external modified ASW solution. After observing the light-dependent channel activity in the cell-attached patch, the patch membrane was excised for the inside-out patch recordings to allow application of cyclic nucleotides to the intracellular face. cGMP opened the channel in the excised patch. This is direct evidence that cGMP is the second messenger that opens the light-dependent K^+ channel in a simple hyperpolarizing photoreceptor, Ip-2 or Ip-1 cell.

MATERIALS AND METHODS

Animals and Preparation of Simple Photoreceptor Cells

Experimental animals, the marine gastropod mollusc *Onchidium verruculatum* weighing 10 g or so, were collected from the intertidal zone of Kinko Bay in Sakurajima, Kagoshima, Japan. The animals were kept in a natural seawater aquarium (20–23°C) bubbled with air for 1–2 mo without feeding. The circumesophageal ganglia were exposed by dissecting through the middorsal surface of the mollusc and were isolated after the overlying connective tissue had been removed. This allowed the cell bodies of neurons in the ganglia to be visualized. In this study, we used simple photoreceptor cells, the photoresponsive neurons, Ip-2 and Ip-1, and for comparison, A-P-1 or Es-1 on the same abdominal ganglion. Those cells have been identified previously as shown in Fig. 1 A (Gotow, 1989; Nishi and Gotow, 1992, 1998). No differences in the responses to light could be detected among animals collected in different seasons of the year. To facilitate a tight seal formation between the patch pipette and the cell membrane, the surface of each isolated circumesophageal ganglia (the preparation) was treated with 0.1% Pronase (a nonspecific protease; Calbiochem) in normal artificial seawater (ASW)* (Table I, solution IV) for 5 min, and then rinsed in solution IV without Pronase for 30 min. No differences were noted in the channel properties between enzyme-treated and untreated cells, except for more difficulties in obtaining a tight seal in the later. The preparation was then pinned on the rubber base of a 1-ml recording bath made of Lucite and was perfused continuously with the solutions. This entire procedure as well as that for recording from the cells was performed under dim red light or in total darkness.

Recording and Stimulation

For single channel recordings, standard techniques based on those described by Hamill et al. (1981) were used. Briefly, the patch pipettes were pulled from 1.5 mm outside diameter borosilicate capillaries and were fire polished. In some experiments, the tips of the patch pipettes were coated with Sylgard to reduce the electrical capacitance. They had resistances of between 2 and 2.5 MΩ when filled with solution I or II (Table I). Only patches forming seals >10 GΩ were used for the experiments. Single-channel currents were recorded in the cell-attached and the inside-out patch modes. For a cell-attached recording, the potential difference across the patch membrane (Vm) is the difference between the resting potential of the cell (Vw) and the potential applied to the inside of the pipette (Vp), i.e., Vm = Vw − Vp. Before obtaining the seals on the intact cell, external normal ASW (solution IV containing 10 mM K^+) in the bath was replaced with a modified ASW (solution III containing 150 mM-K^+). When the preparations were perfused and equilibrated with this solution (III) for 1–2 h before commencing the experiments, a constant resting membrane potential (Vw), the mean value of -14 ± 0.2 mV (mean ± SEM, $n = 20$) was obtained from Ip-2 or Ip-1 cells using intracellular microelectrodes. It was expected that this value would be nearly equal to a K^+ equilibrium potential (E_K) because of a relatively high K^+ conductance of the resting membrane and that this estimates the intracellular K concentration, $[K^+]_i$ of ~260 mM from the Nernst equation for K^+. This expectation will be confirmed as shown later (see RESULTS). Solution III also contained 200 mM Mg^{2+}, so that it blocked any synaptic input to the cell (Gotow and Hashimura, 1981). For comparison, Vw of the other simple A-P-1 cells in the 150 mM-K^+ solution (III) showed a constant resting potential, the mean value of -20 ± 0.2 mV (mean ± SEM, $n = 20$) and $[K^+]_i$ in A-P-1 was thus estimated to be ~330 mM in a similar way (Gotow et al., 1994). For an inside-out patch recording, the bath was fully perfused with a 260-mM K^+ pseudointernal solution (solution V) before excising the patch, and then the patch was excised.

Additionally, some whole-cell recordings of membrane voltage and current were made using conventional current- and voltage-clamped techniques with two intracellular microelectrodes.

The bath solution was grounded through an agar/Ag-AgCl bridge containing 1 M KCl, so that the solution change produced a negligible liquid junction potential. The potential of the patch pipette connected with a Ag-AgCl wire was clamped at the desired levels. In this paper, inward currents across the patch membrane are shown conventionally as downward deflections of the current trace.

**Abbreviations used this paper:* ASW, artificial seawater; 8-Br-cAMP, 8-Bromo-cyclic AMP; 8-Br-cGMP, 8-Bromo-cyclic GMP; GC, guanylate cyclase; IP_3, inositol trisphosphate; PDE, phosphodiesterase.

TABLE I

Solutions

	Solution	KCl	NaCl	$CaCl_2$	$MgCl_2$	Sucrose	Tris	HEPES	pH	EGTA
I	450 mM K^+	450	10	10	50	—	10	—	7.8	—
II	200 mM K^+	200	260	10	50	—	10	—	7.8	—
III	150 mM K^+, high Mg^{2+}	150	10	10	200	130	10	—	7.8	—
IV	Normal ASW	10	450	10	50	—	10	—	7.8	—
V	Internal 260 mM K^+	260	50	1	2	408	—	10	7.4	1.5
VI	Internal 330 mM K^+	330	50	1	2	287	—	10	7.4	1.5

The pH of solutions was adjusted with HCl for solutions I–IV and with NaOH for solutions V and VI to the indicated values. Sucrose was added to maintain the isotonicity of the solution. The free Ca^{2+} in solutions V and VI was designed to obtain about 10^{-7} M (pCa = 7).

Test drugs applied to the cytoplasmic face of inside-out patches were cAMP, cGMP obtained from Sigma-Aldrich, and 8-Br-cAMP and 8-Br-cGMP obtained from Alexis Biochemicals Corp. The drugs were simply dissolved in the perfusing solution V.

White or monochromatic light from a tungsten quartz-iodide lamp (6.3 V, 45 W) was used for illumination. The monochromatic light was focused through a grating monochromator (Shimadzu Bausch and Lomb) with a half width of 5 nm, but the white light was focused directly. The light, focused to a spot of 4 mm in diameter, was transmitted to the preparation via a fiber-optic light guide (5 mm in diameter). A previous spectral study showed a single peak sensitivity of 510 nm light for Ip-2 or Ip-1 (Nishi and Gotow, 1998). The light stimulation of 510 nm was thus used for most of the experiments unless otherwise indicated. An electromagnetic shutter was used to control the stimulus duration. The light intensity was reduced as desired with neutral-density filters. The light intensity (log I) was expressed as a relative log unit of the attenuation by the filter, so that the log I of the unattenuated light was taken as 0 log unit. The unattenuated intensity at 510 nm was 7.2×10^{-5} W/cm^2 or 1.8×10^{14} photon/cm^2 · s, below the maximum intensity required to saturate the macroscopic hyperpolarizing response. The radiant energy flux (the absolute intensity of light) was measured with a radiometer (Model 4090; SJI) whose sensor was placed at the position of the cell.

Solutions

The pipette and bath solutions are given in Table I. Patch pipettes were filled with a 450-mM K^+ solution (solution I) or a 200-mM K^+ solution (solution II, Na^+ was substituted for K^+). In two or three experiments for the inside-out patch recording, solution V in the perfusing bath was replaced with a 330-mM K^+ pseudointernal solution (solution VI), according to $[K^+]_i$ of 330 mM for A-P-1. The bath solution could be changed in <1 min by the present perfusing system. All bath solutions were kept at 22–24°C.

Data Collection and Analysis

Single-channel current signals were recorded using a patch clamp amplifier (CEZ-2300; Nihon Kohden) and stored together with the voltage signal on a video-cassette recording system (VR-10B; Instrutech) for later analyses. The data were filtered at 1 KHz by a 4-pole Bessel low-pass filter and digitized at 10 KHz using Digidata 1200A (Axon Instruments, Inc.), controlled by Axoscope 1.1.2 (Axon Instruments, Inc.), although only a trace (Fig. 1 D) was low-pass filtered at 0.5 KHz.

Amplitude histograms were constructed from the digitized current data. These histograms were then fitted with two Gaussian distributions, using Levenberg-Marquardt algorithm as implemented in pClamp 6.0.4 (Axon Instruments, Inc.). The single-channel current and the open probability (Po) were determined by analyzing amplitude histograms normalized to a total area. Histograms of open time were constructed after setting the transition threshold to the average (midway) of the closed and open current levels. For open and closed time histograms, events shorter than 0.2 ms were excluded from the exponential fitting because of the high frequency limit of the experimental systems and low-pass filters (fc = 1 KHz). No correction was made for the missed events shorter than 0.2 ms owing to the limitation of time resolution. Open and closed histograms were fitted by the sum of two exponentials by Simplex algorithms in pClamp 6.0.4 (Axon Instruments, Inc.). Measurements are given as mean ± SEM; n = number of patches analyzed on different cells, and statistical significance was tested using Student's t test.

Mean open and closed times, τ_o and τ_c, were calculated as weighted averages of two open or two closed time constants, i.e.,

$$\tau_i = (A_{i1}\tau_{i1} + A_{i2}\tau_{i2})/(A_{i1} + A_{i2}), \quad i = o \text{ or } c, \tag{1}$$

where A_{i1} and A_{i2} are the areas under the best-fit short and long exponential components of the open (i = o) and closed (i = c) time distributions, and τ_{i1} and τ_{i2} are their time constants.

P_Os determined as described above were smaller than P_Os estimated as $\tau_o/(\tau_o + \tau_c)$, in the case of light activated channels, whose activities has the early and late phases. The late phase has a small number of very long closed periods over seconds and those periods were neglected in the exponential curve fittings to determine τ_{c2} and so in the latter estimation of Po. However, dependency of P_Os on light intensity and membrane voltage (Vm) were unchanged. Two kinds of P_Os of the cGMP-activated channels were similar due to lack of the late phase. We adopted the former P_O due to smallness of their errors (SEMs).

RESULTS

The Light-dependent Channels in Intact Simple Photoreceptors

Extraocular photoreceptors, the photoresponsive neurons, Ip-2, Ip-1, A-P-1, and Es-1, examined in this study are located on the dorsal aspect of the *Onchidium* abdominal ganglion (Fig. 1 A). These neurons were referred as a simple photoreceptor cell, for lack of any morphological features such as microvilli and cilia (Nishi and Gotow, 1998; also see INTRODUCTION).

The simple Ip-2 or Ip-1 responds to light with a hyperpolarizing receptor potential, caused by an increase in K^+ conductance (Nishi and Gotow, 1998), whereas a

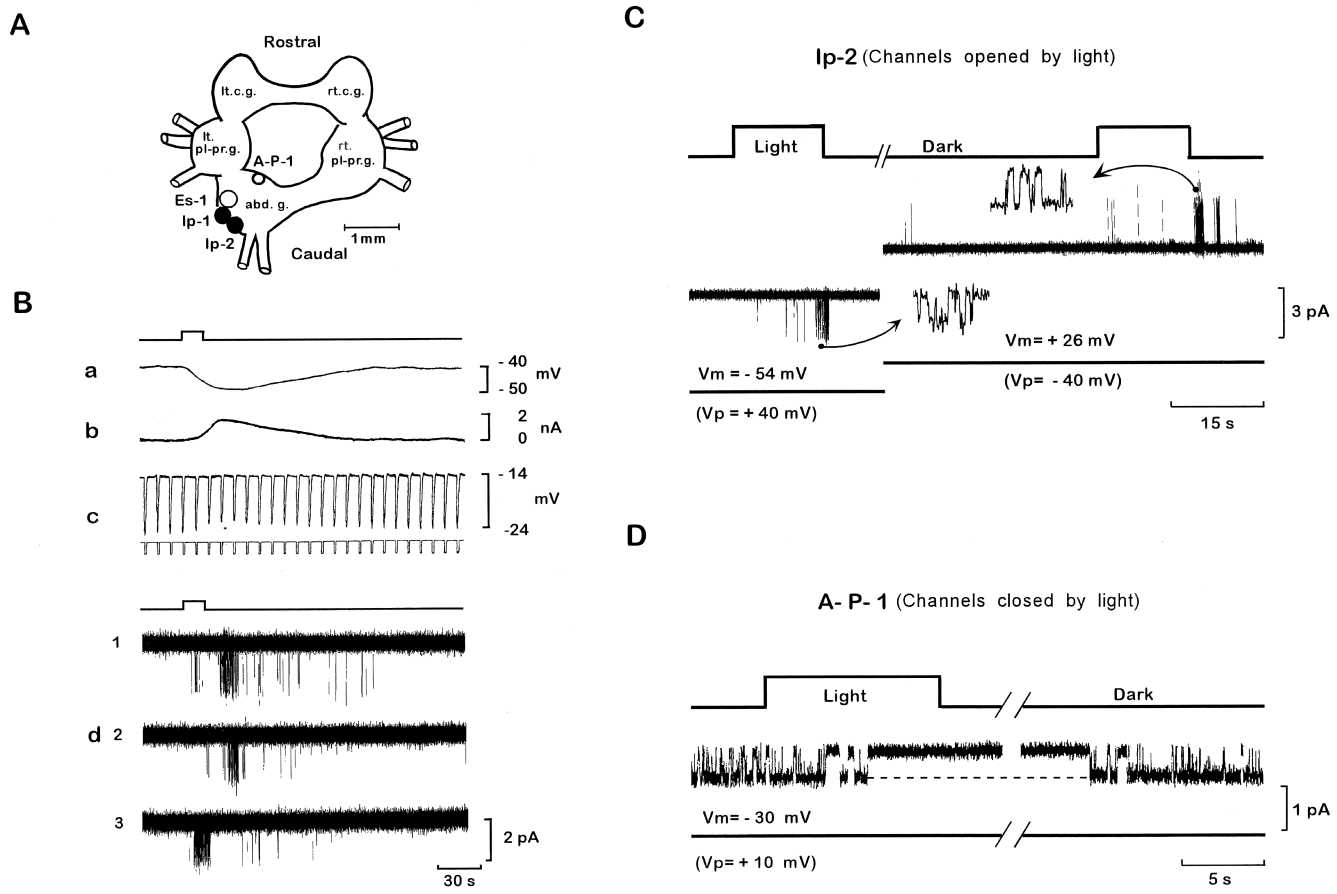

FIGURE 1. (A) A sketch of the dorsal surface of the circumesophageal ganglia, showing approximate positions of the somata of photoresponsive neurons, Ip-1 and Ip-2, and for comparison, A-P-1 and Es-1, which locate on the abdominal ganglion (abd. g.). lt. c. g. and rt. c. g. are the left and right cerebral ganglia, and lt. pl-pr. g. and rt. pl-pr. g., the left and right pleuro-parietal ganglia. (B) Macroscopic (a–c) and microscopic (d) photoresponses of Ip-2 cell. Each upward step trace above a and d1 shows the timing of identical 15-s stimuli of a moderate white light (3×10^{-3} W/cm^2) and was repeated after dark adaptation. (a) A hyperpolarizing receptor potential. (b) A hyperpolarizing receptor current when voltage-clamped at −40 mV. (c) A photoresponse indicating an increase in membrane conductance of the cell bathed in a modified ASW. Identical current pulses (2 nA, 1 s duration) were delivered to the cell at 0.2 Hz (a current record under trace c) and the potential change was recorded in trace c. Each trace (a–c) is shown using a real time recorder filtered at 5 Hz. (d1, 2, 3) The single-channel current activity using a 450-mM K^+-filled pipette, low-pass filtered at 1 KHz and digitized at 10 KHz. (C) Light-dependent single-channel recordings from a cell-attached patch of Ip-2, with a 200 mM-K^+-filled pipette (middle trace). The top trace shows the timings of the same 15 s light stimuli as in B. The bottom trace shows the change in membrane potential (Vm). The expanded traces in two insets show the inward and outward currents composed of unitary currents. (D) Single-channel currents closed by light in a cell-attached patch of A-P-1, using a 200 mM-K^+-filled pipette (middle trace). This was shown for comparison with the channels of Ip-2 opened by light in B and C. The upper trace shows the timing of 10 s stimulus of a saturating white light (3×10^{-3} W/cm^2, the same intensity as in C and D). A dotted line in the middle trace shows the open channel level.

depolarizing photoresponse of the simple A-P-1 or Es-1 results from closing the light-dependent K^+ channel (Gotow et al., 1994).

Fig. 1 B shows the hyperpolarizing macroscopic voltage (a) and current (b) photoresponses of Ip-2 bathed in the normal ASW (solution IV). When Ip-2 was voltage-clamped at nearly the resting potential, −40 mV, the macroscopic outward photocurrent showed a slow monophasic wave which reached a peak in 20–30 s and then returned more slowly to the dark level within ~2 min with a time course similar to that of the macroscopic hyperpolarizing voltage response at the same membrane potential (Fig. 1 B, a and b). A similar slow monophasic waveform to these voltage or current photoresponses was reproducibly obtained, when the same identical 15 s stimuli of moderate light intensity were repeated at 5-min intervals after 30 min of dark adaptation. Such a voltage or current waveform was also graded with light intensity (unpublished data).

For the present cell-attached recordings the external solution (IV) was replaced with modified ASW (solution III containing 150 mM-K^+). As expected, the membrane potential (Vw) of Ip-2 exposed to solution III remained constant, at approximately −14 mV despite the

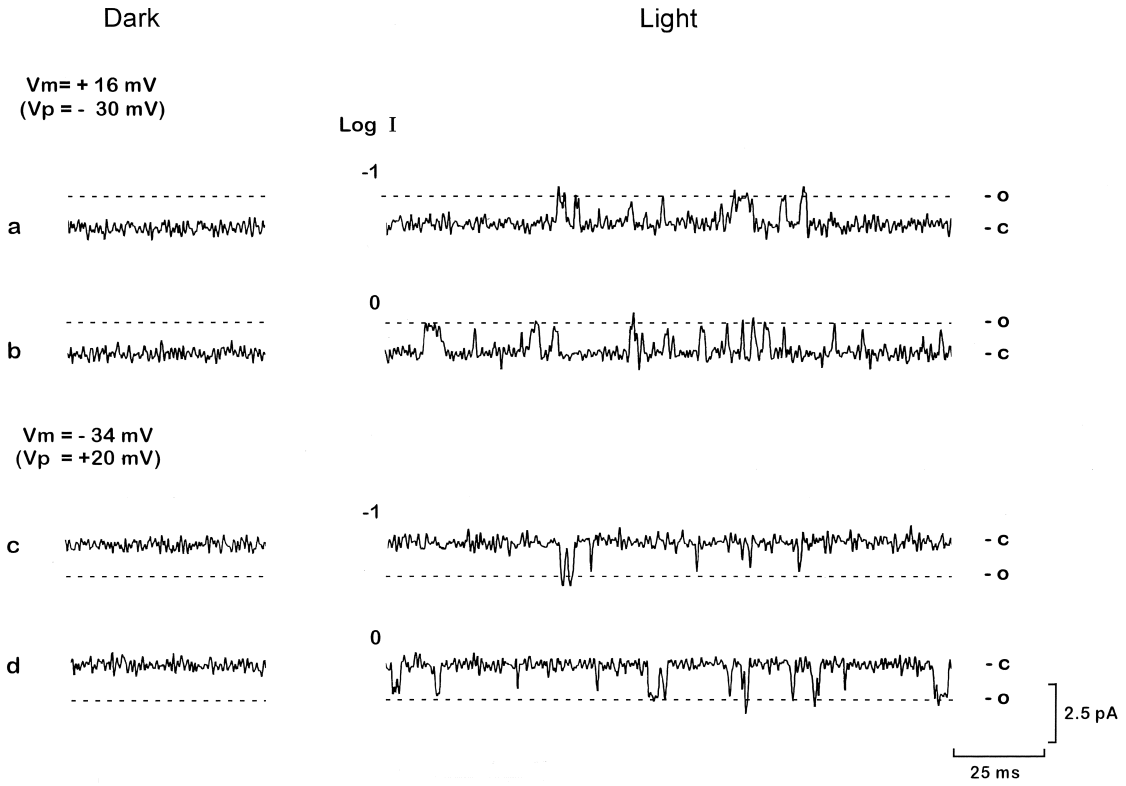

FIGURE 2. Effects of light intensity on the light-dependent channel activities. Each single-channel current activity was recorded from a cell-attached patch on Ip-2 cell, using the pipette filled with 200 mM K^+. Left side traces in the dark show the lack of channel activity at Vm = 16 mV (Vp = −30 mV) and Vm = −34 mV (Vp = 20 mV). Right side traces: effects of relative log light intensity (Log I), −1 (a) and 0 (b) at Vm = 16 mV, and −1 (c) and 0 (d) at Vm = −34 mV, using 510 nm light. The dashed lines show the outward (a and b) and inward (c and d) single-channel current-levels when the light-dependent channel was opened. Each light-dependent channel activity shows the early phase activated by 15 s light stimuli of each identified intensity. All data were low-pass filtered at 1 KHz and digitized at 10 KHz in this and the following figures.

light stimulation (Fig. 1 B, c). However, this membrane responded to the light with an apparent increase in membrane conductance (Fig. 1 B, c) that had a time course similar to that of the macroscopic photoresponse (Fig. 1 B, b) in the normal ASW. This was indicated by a decrease in the amplitude of electrotonic potentials produced by periodic constant current pulses (a trace under Fig. 1 B, c). These observations were confirmed in 13 other Ip-2 or Ip-1 cells. These results supported our assumption that Vw of −14 mV is equal to E_K (calculated to be −14.1 mV at 23°C), equilibrating the external K^+ of 150 mM and $[K^+]_i$ of 260 mM, so that Vw bathed in solution III remains constant regardless of the macroscopic photoresponse if it is K^+ selective, as if the cell were voltage clamped. Thus, a replacement of the normal ASW with solution III was conducted to maintain Vw, i.e., a patch membrane potential (Vm), constant during the cell-attached single-channel recordings.

Fig. 1 B, d, is an example of the cell-attached single-channel recordings from the Ip-2 cell under such a condition. In these recordings, the patch membrane potential, Vm, was held at −14 mV because the pipette potential (Vp) was 0 mV, and Vm = −(14 + Vp) mV. As expected, the light-dependent single-channel currents were activated by the same identical 15 s light stimuli as those in the above macroscopic photoresponse. Each of the three sequential stimuli was given at the same intervals of 5 min, chosen to obtain an approximately constant, reproducible macroscopic photoresponse. Each trace showed an activity of the inward single-channel currents that was initially high in different delayed times and then declined to a much lower maintained level over 1 min in a manner roughly similar to that of the macroscopic response. Similar observations were obtained in the following all light-dependent channel recordings studied using this protocol.

Fig. 1 C shows the lack of any significant effect of the membrane potential depolarization on activation of the light-dependent channel currents. The light-dependent single-channel unitary currents (as shown by arrows in an expanded time scale) were inward at Vm of −54 mV (Vp = 40 mV). Conversely, these unitary currents were outward at Vm of 26 mV (Vp = −40 mV). As shown in the middle part of Fig. 1 C, however, no channel current was activated in the dark while Vm was kept

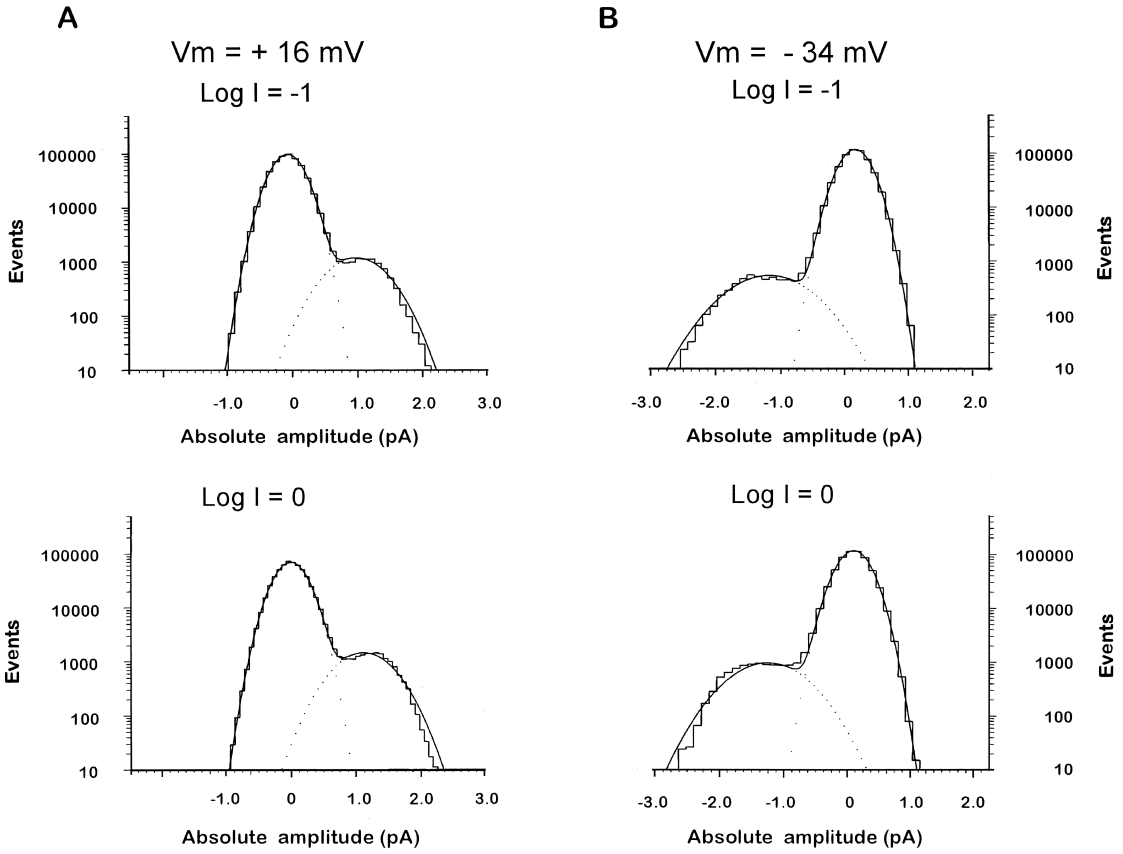

FIGURE 3. Amplitude histograms of the light-dependent channel currents in the same cell-attached patch as shown in Fig. 2, at Vm of 16 (A) and −34 (B) mV. Each histogram was constructed from an entire record for 1 min (containing both the early and late phases) obtained from each of different patches after the light illumination (Log I) of 15 s as in Fig. 2, a–d. The histograms were fitted with the sum of two Gaussian curves, reflecting the existence of only one open channel. The means and SEMs of single-channel current levels and the open-channel probability (P_O) were computed from two distinct Gaussian curves. (A) 1.16 ± 0.003 pA, P_O = 2.2% at −1 (top) and 1.20 ± 0.003 pA, P_O= 3.5% at 0 (bottom). (B) −1.42 ± 0.006 pA, P_O = 0.9% at −1 (top) and −1.35 ± 0.005 pA, P_O = 1.8% at 0 (bottom).

depolarized at a 26 mV beyond the reversal potential (−6.7 mV), although only a sporadic channel activity occurred rarely. This indicates that the activation of the channel by light occurs almost independently of the depolarization. An experiment was continued only if the cell-attached patch contained solely light-dependent channels. On the other hand, the light-dependent channels of Ip-2 or Ip-1 cells opened by light contrast with the light-dependent channels which are active during dark and are closed by light in other depolarizing A-P-1 or Es-1 cells (Fig. 1 D; see also Gotow et al., 1994).

In the present cell-attached recordings, ~20% (>100 patches) of the attempts contained the light-dependent single-channels. Multiple openings of two or more channels were observed in ~20% of their patches and were excluded from the following channel analysis.

Kinetics of the Light-dependent Channel

Effect of light intensity on the light-dependent channel. As shown above, the response of Ip-2 cells to an identical 15 s light usually had an early phase characterized by high channel activity followed by a late phase with declining channel activity over 1 min.

Fig. 2 shows an example of the light-dependent single-channel currents (in the early phase) from an Ip-2 cell-attached patch, elicited by two different light intensities. The reversal potential for K^+ (E_K) of the patch membrane was estimated to be −6.7 mV under 200-mM K^+ (solution II)-filled pipettes (see also Fig. 6). The rectangle-like appearance of definite, unitary channel currents was observed outwardly (a) at Vm of 16 mV and inwardly (c) at Vm of −34 mV in the presence of a moderate light (−1 log I), as expected for a K^+-selective channel. When the light changed to a bright intensity (0 log I), which is less than that required to saturate the macroscopic photoresponse, the activity of these outward and inward channel currents increased (b and d, respectively). The amplitude histograms for the above channel currents (containing both the early and late phases) are shown in Fig. 3. Each histogram showed two distinct Gaussians, reflecting the existence of only the same one open-channel current peak

TABLE II

Comparison of Light-dependent and cGMP-activated Channel Kinetics

Light-dependent channel									
Log I	*n*	Vm	τ_{O1}	τ_{O2}	τ_{O}	τ_{C1}	τ_{C2}	τ_{C}	P_O
		mV	*ms*	*ms*	*ms*	*ms*	*ms*	*ms*	%
−1	4	16	0.51 ± 0.10	2.6 ± 0.2 (0.28 ± 0.02)	1.1 ± 0.1	6.7 ± 2.9	100 ± 20 (0.47 ± 0.05)	52 ± 14	0.83 ± 0.18
0	4	16	0.68 ± 0.10	3.3 ± 0.2 (0.15 ± 0.01)	1.1 ± 0.1	8.8 ± 2.4	86 ± 7 (0.39 ± 0.07)	32 ± 5	2.5 ± 0.3
−1	6	−34	0.60 ± 0.08	2.9 ± 0.2 (0.52 ± 0.14)	1.4 ± 0.2	9.8 ± 1.3	500 ± 20 (0.49 ± 0.13)	240 ± 49	0.48 ± 0.13
0	6	−34	0.57 ± 0.03	3.5 ± 0.6 (0.42 ± 0.09)	1.6 ± 0.3	9.8 ± 1.1	150 ± 30 (0.57 ± 0.10)	90 ± 18	1.5 ± 0.2
cGMP-activated channel									
cGMP									
mM									
0.2	4	20	0.38 ± 0.04	1.8 ± 0.1 (0.26 ± 0.07)	0.75 ± 0.06	3.9 ± 1.0	52 ± 10 (0.50 ± 0.08)	30 ± 9	2.8 ± 0.09
2	4	20	0.38 ± 0.11	3.2 ± 1.0 (0.06 ± 0.02)	0.58 ± 0.21	2.9 ± 0.8	25 ± 2.4 (0.34 ± 0.08)	10 ± 3	11.0 ± 4.1
0.2	5	−30	0.37 ± 0.06	1.9 ± 0.3 (0.17 ± 0.04)	0.61 ± 0.18	9.3 ± 1.5	97 ± 26 (0.52 ± 0.10)	54 ± 18	1.9 ± 0.3
2	4	−30	0.54 ± 0.07	2.5 ± 0.6 (0.08 ± 0.01)	0.71 ± 0.13	5.5 ± 0.2	23 ± 3 (0.42 ± 0.13)	12 ± 1	5.0 ± 0.6

Kinetic parameters for light-dependent and cGMP-activated K^+ channels. The data were obtained from a 200-mM K^+-filled pipette. As described in the text, τ_{O1}, τ_{O2}, and τ_O are short, long, and mean open time constants, respectively; τ_{C1}, τ_{C2}, and τ_C are short, long, and mean closed time constants, respectively. The values in parentheses under τ_{O2} and τ_{C2} show the relative contents of their time constants. P_O shows the open probability of channels. The light intensity (Log I), −1 and 0, show log unit intensities. Values are mean (given in two significant figures) ± SEM. *n*, number of patches tested.

around 1.2 pA at Vm of 16 mV in Fig. 3 A, and around −1.4 pA at Vm = −34 mV in Fig. 3 B. However, as shown in a pair of histograms (A and B), the height of the one Gaussian curve showing the open-channel state increased with the light intensity. This computed that the open probability (P_O) of the channels increases from its initial value of 2.2% (−1 log I) to 3.5% (0 log I) at Vm of 16 mV and from the initial value of 0.9% (−1 log I) to 1.8% (0 log I) at Vm of −34 mV. The mean value (mean ± SEM) for these open probabilities is shown in Table II.

Fig. 4 shows the open and closed time distribution histograms for the same series of records as those in Fig. 2. All histograms could be well fitted by the sum of two exponentials with relative contents of their areas (i.e., relative contents of event numbers, given as decimal values in parentheses), the open time constants τ_{o1}, τ_{o2} and the closed time constants τ_{c1}, τ_{c2}.

Consider first the open time distributions at Vm = 16 mV and −1 log I in Fig. 4 A. The open time constants of the fit had τ_{o1} = 0.47 ms for the short component and τ_{o2} = 2.8 ms for the long component. The mean open time (τ_o) was 1.1 ms in this condition. At the same Vm = 16 mV and higher 0 log I, their constants were 0.78 for τ_{o1}, 3.6 for τ_{o2}, and 1.2 ms for τ_o. As shown in Fig. 4 B, when Vm was hyperpolarized from 16 to −34 mV, the open time distributions gave τ_{o1} = 0.55, τ_{o2} = 3.3, and τ_o = 0.96 ms at −1 log I, and τ_{o1} = 0.62, τ_{o2} = 4.2, and τ_o = 0.91 ms at higher 0 log I. In Table II, the average value (mean ± SEM) for the concerned open time constants is summarized. Very small values of τ_{o1} near the time resolution limit (0.16 ms) of the 1 KHz low-pass filter may not be accurate and may be overestimated (see DISCUSSION). In spite of the inaccuracy, this result showed that the open time constants, τ_{o1}, τ_{o2}, and the mean open time, τ_o, are not significantly different between the two light intensities −1 and 0, and between the two membrane voltages 16 and −34 mV. Namely, differences between any pairs of τ_{o1}, τ_{o2}, and τ_o for the light-dependent channels in Table II are not significant ($P > 0.1$ in a paired Student's *t* test).

Consider next the closed time distributions at the same voltage and light intensity as above in Fig. 4. At Vm = 16 mV and −1 log I, the two closed time constants and the mean closed time were τ_{c1} = 12, τ_{c2} = 130, and τ_c = 64 ms, but at 0 log I, they were 14 for τ_{c1}, 100 for τ_{c2}, and 37 ms for τ_c. When Vm was hyperpolarized from 16 to −34 mV, at −1 log I, the closed time distributions gave τ_{c1} = 11, τ_{c2} = 540, and τ_c = 180 ms, but at higher 0 log I, τ_{c1} = 12, τ_{c2} = 190, and τ_c = 64 ms. The average value (mean ± SEM) for the concerned closed time constants is shown in Table II. This showed that τ_{c1} is not significantly altered by the differences in the membrane voltage and light intensity ($P > 0.1$), whereas both τ_{c2} and τ_c are significantly reduced when light is increased from −1 to 0 log I only at Vm = −34 mV ($P < 0.05$).

Thus, these results show that P_O of the single-channel activity increases with increasing light and also with depolarization, without significant changes in any of τ_{o1}, τ_{o2}, τ_o, or τ_{c1}.

Effect of membrane potential on the light-dependent channel activity. Fig. 5 shows typical examples of the light-dependent single-channel currents of Ip-2 cells at various

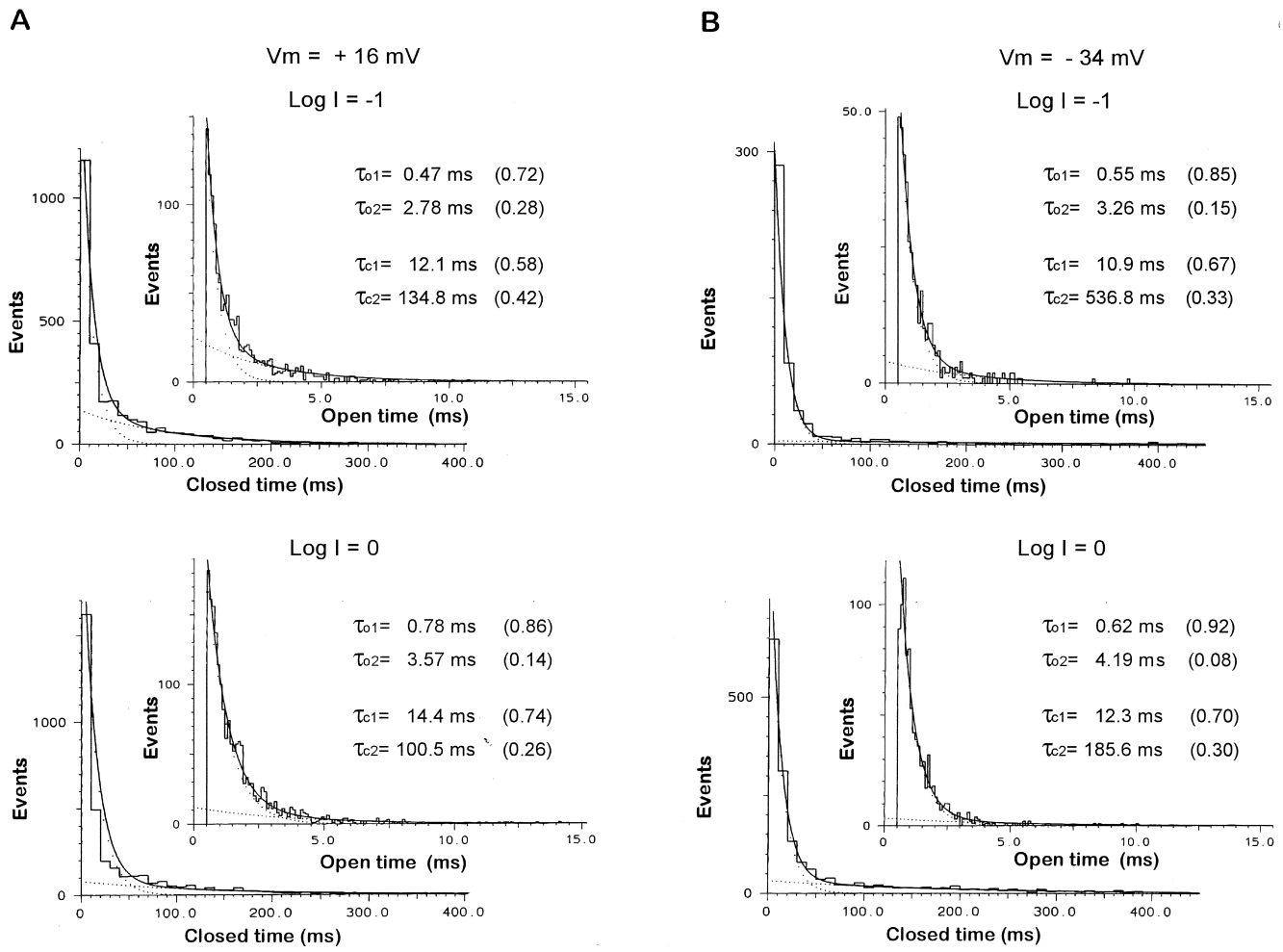

FIGURE 4. Open time and closed time histograms of the light-dependent channel, at Vm of 16 (A) and −34 (B) mV. The data were obtained from the entire record for 1 min containing both the early and late phases of channel activity, after light illumination (Log I) of 15 s in the same patch as in Fig. 2. All the distributions were fitted with sums of two exponentials yielding the indicated relative contents in areas (decimal values, given in parentheses), open time constants τ_{o1} and τ_{o2}, and closed time constants τ_{c1} and τ_{c2}. For other details see text.

membrane potentials, activated by an identical light intensity, 0 log I. Definite, unitary currents in the order of pA were resolved at all depolarizing and hyperpolarizing membrane potentials tested with the 200-mM K^+ (A)- and 450-mM K^+ (B)-filled pipettes. The inward single-channel current in the hyperpolarizing potentials decreased as the membrane was depolarized, and reversed its sign from inward to outward at a more positive potential, as expected from a K^+-selective channel. An analysis for the unitary currents showed that P_O increases progressively with membrane depolarization (Fig. 5 A), in accordance with the results in Table II.

Ionic Selectivity and Conductance of the Light-dependent Channel

Fig. 6 A shows the single-channel current-voltage (i-V) relationships constructed to examine the permeability properties of the light-dependent channels. The data were obtained from experiments of the same type as in Fig. 5. The single-channel current decreased as the membrane was depolarized and reversed at Vm of −14 ± 0.9 mV (mean ± SEM, $n = 5$) in the 450-mM K^+ pipette (filled circles) and at Vm of −6.8 ± 0.4 mV (mean ± SEM, $n = 10$) in the 200-mM K^+ pipettes (open circles). The intracellular K^+ concentration was estimated to be 260 mM from the Nernst potential of about −14 mV as shown in MATERIALS AND METHODS and Fig. 6 C. From this estimate, if the single-channel current is K^+ selective, it should reverse at a patch membrane potential (Vm) of ~14.1 mV in the 450-mM K^+ and at Vm of about −6.7 mV in the 200-mM K^+ pipettes, which correspond to E_K of the patch membrane predicted by the Nernst equation. Thus, both the two reversal potentials measured above were very close to the theoretical prediction for E_K. This suggests that the

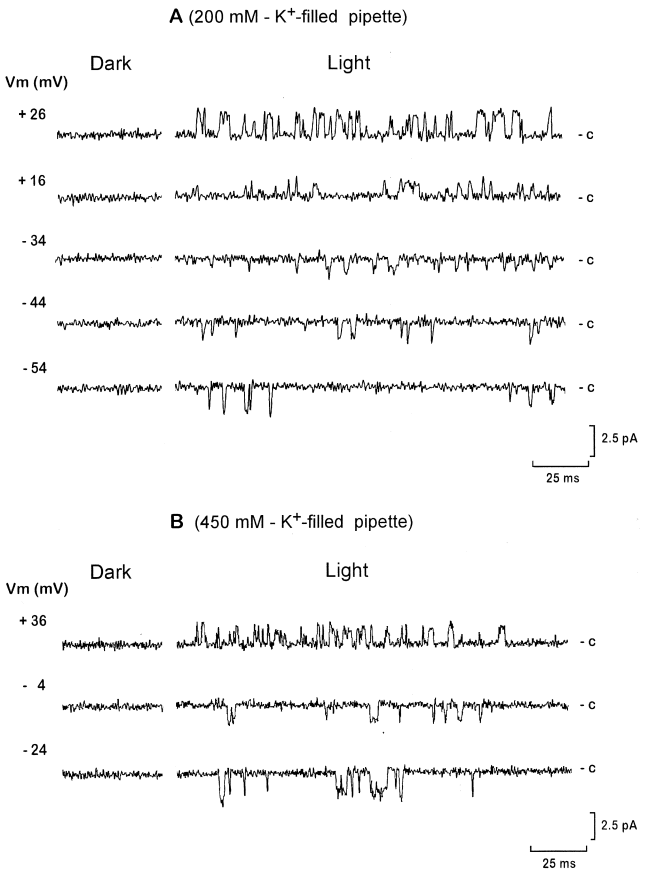

FIGURE 5. Effects of membrane potential on the light-dependent channel currents using 200-mM (A) and 450-mM (B) K^+-filled pipettes. Records in A and B were obtained from different Ip-2 cells. The channels were activated by an identical 0 light stimulus for 15 s at 510 nm, delivered at 5-min intervals while the membrane potential (Vm) was held at each of the indicated values in the dark. Left column traces in the dark show the lack of channel activity at various Vms. Closed channel states (-c) are shown on the right of each trace. In A, the open probability (P_O) of the light-dependent channels at each given Vm was computed from the data for 1 min after the light stimulus: P_O = 2.5% at Vm = 26, 2.0% at 16, 1.5% at −34, 0.8% at −44, and 0.4% at −54 mV.

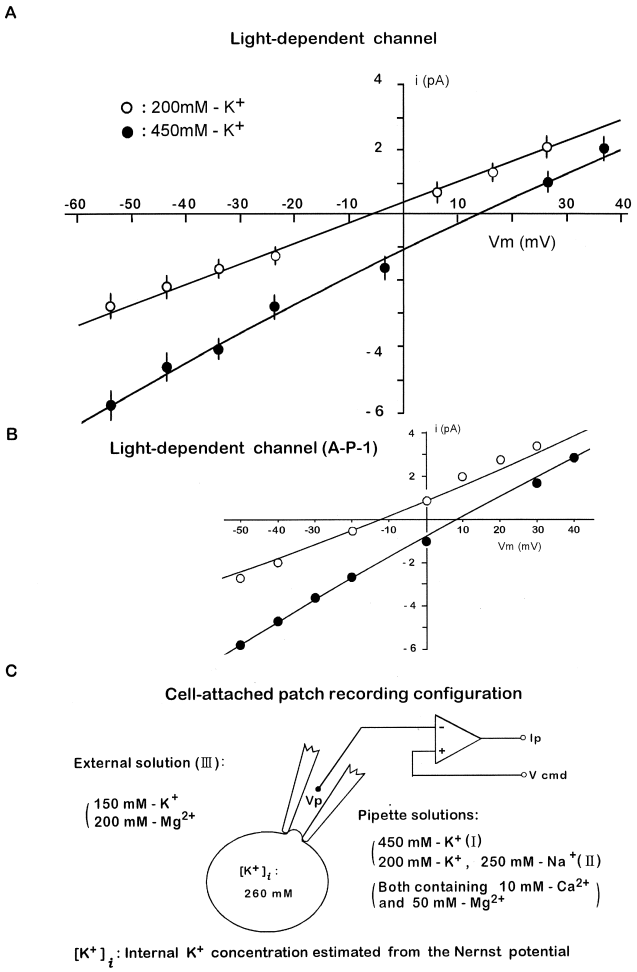

FIGURE 6. (A) i-V relations of the light-dependent single-channel currents using 200-mM (○) and 450-mM (●) K^+-filled pipettes. The data were obtained from experiments of the same series of Ip-2 cells as shown in Fig. 5. Inward channel currents across the patch membrane are shown as negative in the ordinate. Vm in the abscissa corresponds to (Vw-Vp) mV; Vw = −14 mV. Reversal potentials, Vm = −6.8 ± 0.4 mV (mean ± SEM, n = 10) with 200-mM K^+ and 14 ± 0.9 mV (mean ± SEM, n = 5) with 450-mM K^+ pipettes. The slope conductances were 62 (200 mM K^+) and 91 pS (450 mM K^+) around at Vm = 0. Symbols indicate the mean and vertical bars ± SEM. The data points are the mean (the symbol) ± SEM (the vertical bar) of 5–10 patches. The solid curves are the best-fit curves of the GHK equation (Eq. 2). (B) i-V relations of the light-dependent channel currents of A-P-1 cells. In this cell, Vw = −20 mV and the estimated $[K^+]_i$ is 330 mM. Each data point was obtained from our published paper (Gotow et al., 1994), and it shows the mean of four separate patches. The lines through the points are the best-fit lines of the GHK equation (Eq. 2), for details see text. (C) A sketch map showing the experimental conditions underlying the cell-attached recordings to obtain the i-V relations in A.

light-dependent single-channel current is primarily K^+ selective. Related matters will be discussed later.

The above two i-V relations for the light-dependent K^+ channels were also predicted by the Goldman-Hodgkin-Katz (GHK) equation (Hodgkin and Katz, 1949),

$$I_K = P_K F^2 V([K^+]_i \exp[VF/RT] - [K^+]_O) / RT(\exp[VF/RT] - 1), \quad (2)$$

where R, T, and F have their usual meanings. If we put $[K^+]_i$ = 260 mM and V, i.e., Vm = −(Vp + 14) mV, an estimate of the K^+ permeability, P_K(cm^3/s) of 6.8 × 10^{-14} at $[K^+]_o$ of 200 mM in solution II and 6.2 × 10^{-14} cm^3/s at $[K^+]_o$ of 450 mM in solution I, gave the best-fit curves along the experimental data points in Fig. 6 A.

Our previous paper showed that the depolarizing photoresponses of another simple photoreceptor, A-P-1 cells, resulted from closing of the light-dependent K^+

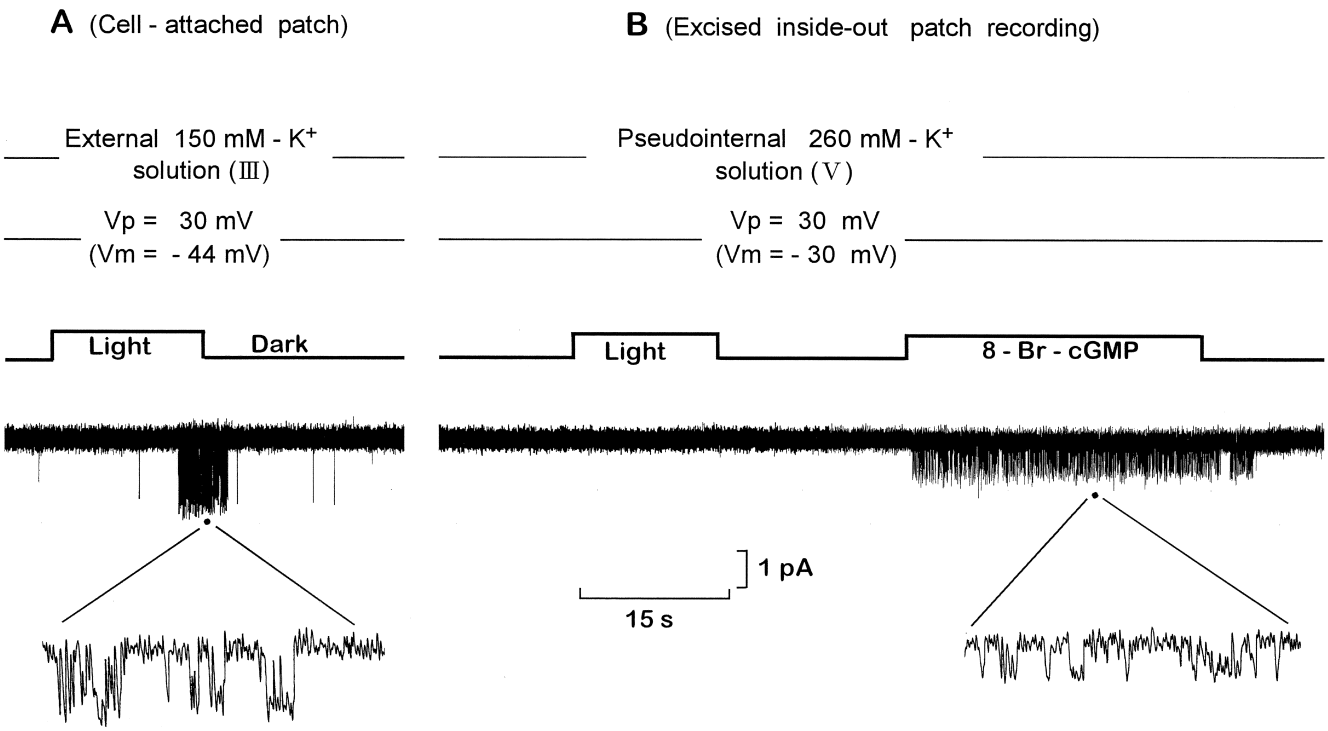

FIGURE 7. A chart of recording showing a series of changes from the cell-attached patch (A) to the inside-out patch (B) excised from the intact Ip-2 cell. A and B are continuous recordings using the same 200-mM K^+-filled pipette. The bottom in A shows light-dependent single-channel currents bathed in a 150-mM K^+ solution (III) shown above the traces, and the bottom in B, cGMP-activated single-channels, but no light-dependent channels in the excised inside-out patch bathed in a 260-mM K^+ solution (V). The upward steps of the upper trace in A and B show the timings of 15 s stimuli of a saturating white light (3×10^{-2} W/cm^2), and the timing of 30-s application of 0.1 mM 8-Br-cGMP. Parts of the channel recordings at the point marks are shown on the expanded time scale. Note the difference in the driving force under cell-attached (Vm = −44 mV) and inside-out (Vm = −30 mV) modes, though in both A and B Vp was the same 30 mV.

channel (Gotow et al., 1994). Interestingly, we found here that both i-V relations for this light-dependent channel current in A-P-1 cells are also well fitted by Eq. 2, if we use the same two P_Ks as those at $[K^+]_o$ of 200 mM and 450 mM in Ip-2 cells, and replace $[K^+]_i$ of 260 mM and V of −(Vp + 14) mV by 330 mM and −(Vp + 20) mV in A-P-1 cells (Fig. 6 B). In addition, P_O also increased with depolarization, similar to that of Ip-2 cells (Gotow et al., 1994).

Thus, it is suggested that the light-dependent K^+ channels of Ip-2 cells (opened by light) are identical to those of A-P-1 cells (closed by light), on the basis of similar K^+ selectivity, P_K, and voltage-dependence of Po.

On the other hand, the slope channel conductance determined in the voltage range at nearly Vm = 0 mV in the I-V relations of Fig. 6 A, was 91 ± 2.7 pS (mean ± SEM, n = 5) at $[K^+]_o$ of 450 mM and 62 ± 1.3 pS (mean ± SEM, n = 10) at $[K^+]_o$ of 200 mM. For comparison, the concerned single channel conductances in A-P-1 cells determined from the slopes of experimental points were 100 pS (450 mM) and 71 pS ($[K^+]_o$ of 200 mM), 10% larger than those of the light-dependent channel in Ip-2 cells (Gotow et al., 1994).

However, these differences in conductance between Ip-2 and A-P-1 cells can be simply explained by the difference in $[K^+]_i$ of 260 and 330 mM in the following slope equation (Eq. 3), as described below.

This equation (Eq. 3) is obtained by differentiating the GHK equation (Eq. 2) and putting $V \rightarrow 0$,

$$(dI_K/dV)_{V \rightarrow 0} = P_K F^2([K^+]_i + [K^+]_O)/2RT. \quad (3)$$

Using the concerned values for P_K and $[K^+]_o$ common to Ip-2 and A-P-1 cells, but replacing $[K^+]_i$ of 260 mM in Ip-2 with 330 mM in A-P-1 cells, we obtain 93.9 pS (450 mM) and 71.5 pS ($[K^+]_o$ of 200 mM) for the conductance of A-P-1 cells. As expected, these estimated conductance values were in good agreement with the above experimental values for the conductances of A-P-1 cells, within the range of error.

The cGMP-activated Channels in the Inside-Out Patch Excised from the Intact Cells

In the simple A-P-1 cells, we suggested that light activates phosphodiesterase (PDE) to reduce internal cGMP levels and closes the light-dependent K^+ channel activated by their cGMP, a second messenger, thereby

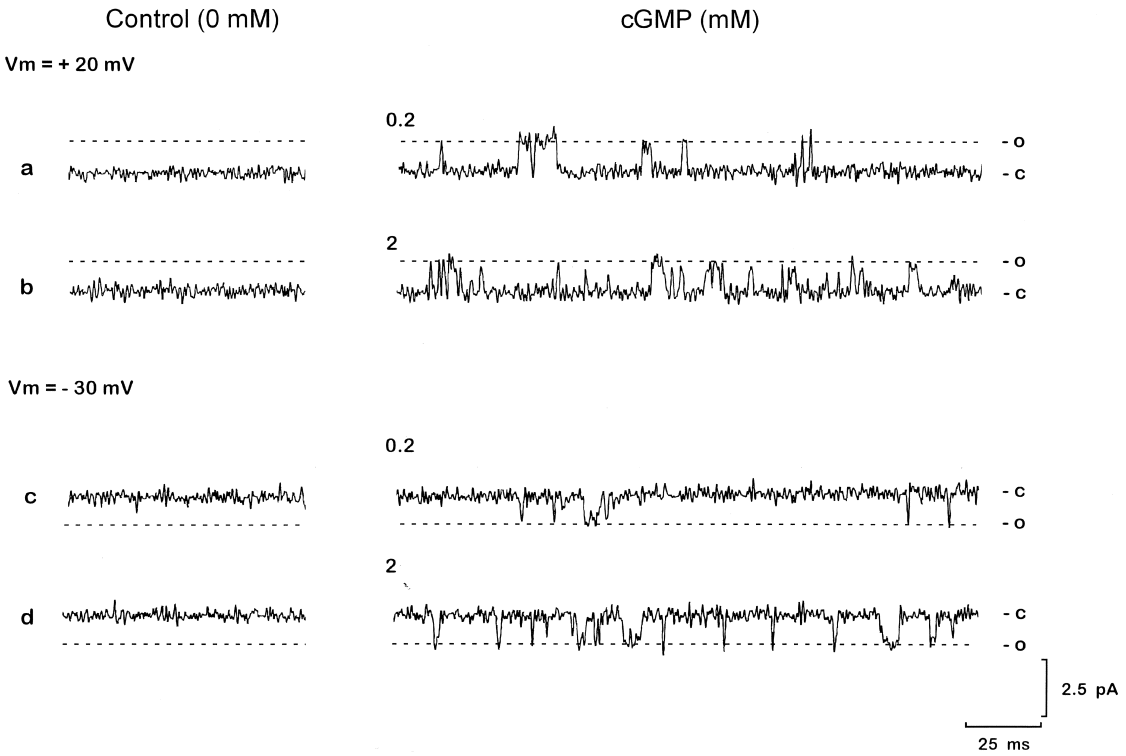

FIGURE 8. Activation of channels in the inside-out patch by cGMP application. The inside-out patch was excised from the intact Ip-2 cell after recording the light-dependent channels, using 200-mM K^+-filled pipette. Open and closed channel states are shown on the right of each trace. The dashed lines show outward (a and b) and inward (c and d) single-channel current levels when the channel was opened. Left side traces in control (0 mM cGMP) show the lack of channel activity at Vm = 20 and −30 mV. Right side traces: channel activation by cGMP of 0.2 (a and c) and 2 (b and d) mM at Vm = 20 and −30 mV, respectively. Each channel activity was obtained during an application of a given cGMP.

leading to the depolarization (Nishi and Gotow, 1989; Gotow et al., 1994). However, in the simple Ip-2 or Ip-1 cells, our recent work (Nishi and Gotow, 1998) has suggested that light activates guanylate cyclase (GC) to increase internal cGMP levels and their cGMP is also a second messenger activating the macroscopic K^+ conductance, being responsible for the hyperpolarization.

To prove whether cGMP can directly activate the light-dependent K^+ channel in the cell-attached patches of Ip-2 cells, we applied cGMP or its analogue to the cytoplasmic side of the excised inside-out patches. After confirming that one light-dependent channel activity was reproducibly observed, the patch membrane was excised into an inside-out patch mode. Patches with overlapping openings of two or more channels dependent on light were excluded from excision.

An example of such an experiment at Vp = 30 mV (Vm = −44 mV) is shown in Fig. 7. A light-dependent single-channel activity was evoked by identical 15 s light stimuli in a cell-attached recording bathed in solution III (Fig. 7 A). Such an activation of single-channel by light was repetitively checked. The membrane depolarization (usually up to Vm of 30 mV) also produced no channel activity (see Fig. 8, a and b). After replacing solution III with solution V, the patch membrane was excised into an inside-out mode. This excised inside-out patch was silent, regardless of dark or light condition (Fig. 7 B). However, when 8-Br-cGMP (hydrolysis-resistant analogs of cGMP) of 0.1 mM was applied to solution V, only one open-channel activity reappeared, as in the cell-attached patch recording before excision, and the activity disappeared on removal of 8-Br-cGMP (Fig. 7 B). As shown here, the channel activation by 8-Br-cGMP or cGMP was maintained relatively uniform over the entire period of the application of 30 s or 1 min, unlike that of the light-dependent channels, and was reproducible without desensitization. An appreciable reduction of ~40% of the single-channel current amplitudes after excision could be explained by 38% reduction of the driving potentials of the channel, from −(14 + 30) − (−6.7) = −37.3 mV to −30 − (−6.7) = −23.3 mV, due to change in Vw from −14 to 0 mV by excision, if the channel is K^+ selective. In this and other similar excised patches, an activation of channel was readily detected by application of just 0.01 mM 8-Br-

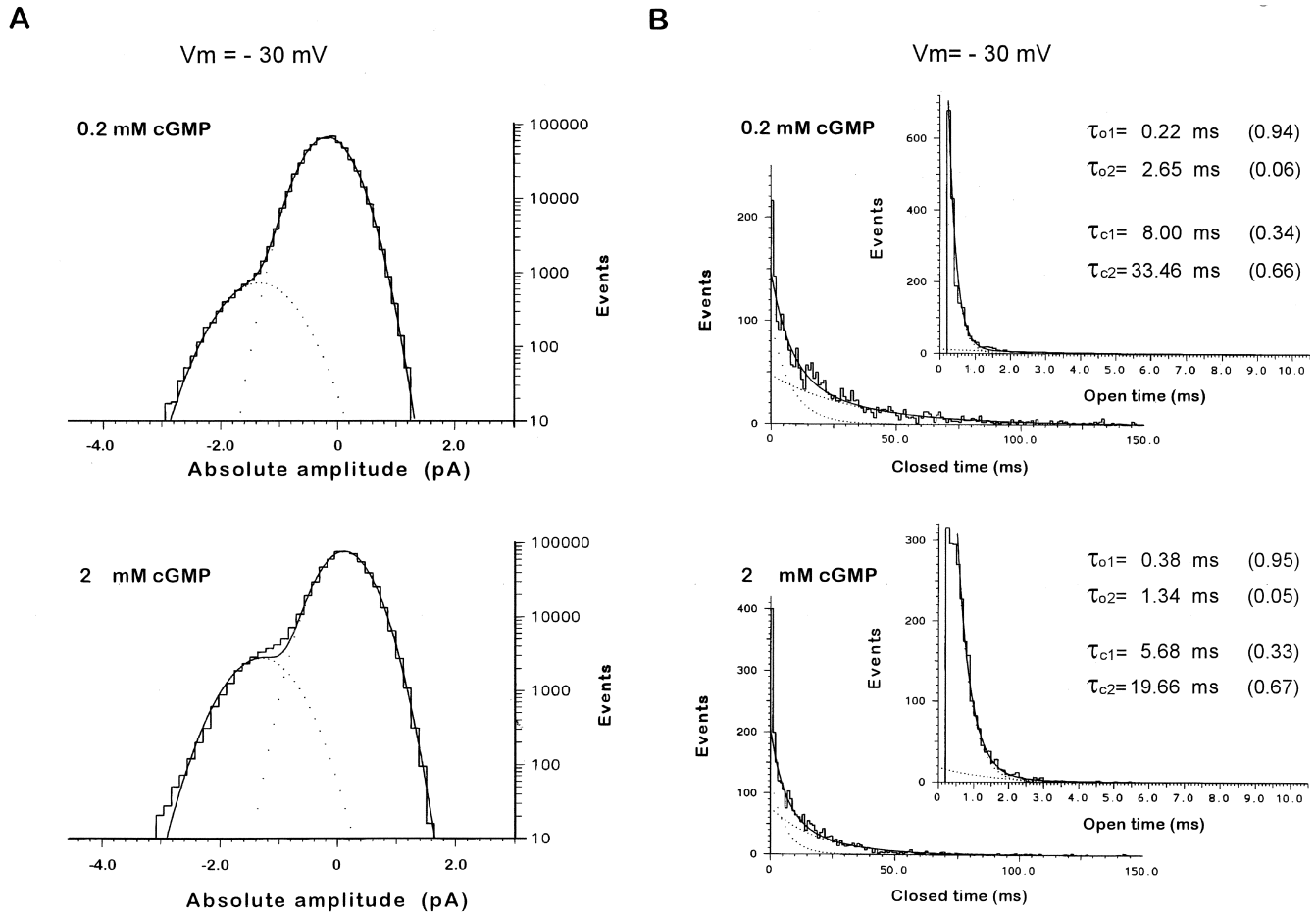

FIGURE 9. (A) Semilogarithmic plots of amplitude histograms of the cGMP-activated single-channel currents at Vm = −30 mV. Each histogram was constructed from the entire runs for 1 min of the same data during cGMP application of 0.2 mM (top) and 2 mM (bottom) as in c and d of Fig. 8, respectively. The histograms were fitted with the sum of two Gaussians, reflecting the existence of only one open-channel current. The single-channel current levels, −1.17 ± 0.005 pA (mean ± SEM) and the open-channel probability, P_O, 1.5% were computed at cGMP of 0.2 mM. At cGMP of 2 mM, −1.23 ± 0.002 pA (mean ± SEM) and P_O = 5.9%. (B) Open time and closed time distribution histograms of the cGMP-activated single-channel currents at Vm = −30 mV. Data were obtained from the entire runs for 1 min during the cGMP application of 0.2 mM (top) and 2 mM (bottom) in the same patch as in Fig. 8. Two open and closed time distributions were fitted with sums of two exponentials yielding the indicated relative contents of areas (parentheses), open time constants τ_{o1} and τ_{o2}, and closed time constants τ_{c1} and τ_{c2}. For other details see text.

cGMP. The channel was also observed with hydrolyzable cGMP, although higher concentrations were required beyond ~0.2 mM, as shown in Fig. 8. However, an application of 0.1 mM 8-Br-cAMP or cAMP at concentrations as high as 2 mM and 1 mM Ca^{2+} to the excised patches failed to activate any channels (not depicted).

About 80% (23 patches) of the present successful inside-out patches always showed only one open-channel activity by application of cGMP or 8-Br-cGMP, consistent with that in the cell-attached patches before excision. In some rare cases, the excised membrane had spontaneous channel activity or was unresponsive to cGMP.

Fig. 8 shows an activation of single-channel by cGMP at different concentrations in the inside-out patch obtained using a similar procedure. As predicted, single-channel currents were activated outwardly (a and b) at Vm = 20 mV, and inwardly (c and d) at −30 mV by cGMP of 0.2 mM (a and c) and 2 mM (b and d). Fig. 9 shows the amplitude histograms (A), and the open and closed time histograms (B) for these cGMP-activated single-channel currents at Vm = −30 mV.

In Fig. 9 A, each amplitude histogram fitted with two distinct Gaussians showed the existence of only the same one channel current peak around −1.2 pA at both cGMP of 0.2 and 2 mM. However, the height of each on the left sides of the two fitted Gaussians increased at 2 mM more than at 0.2 mM cGMP, computing that the open probability, P_O, of the cGMP-activated channels rose from the initial value of 1.5% to 5.9%. The averaged values (mean ± SEM) for P_Os at Vm of

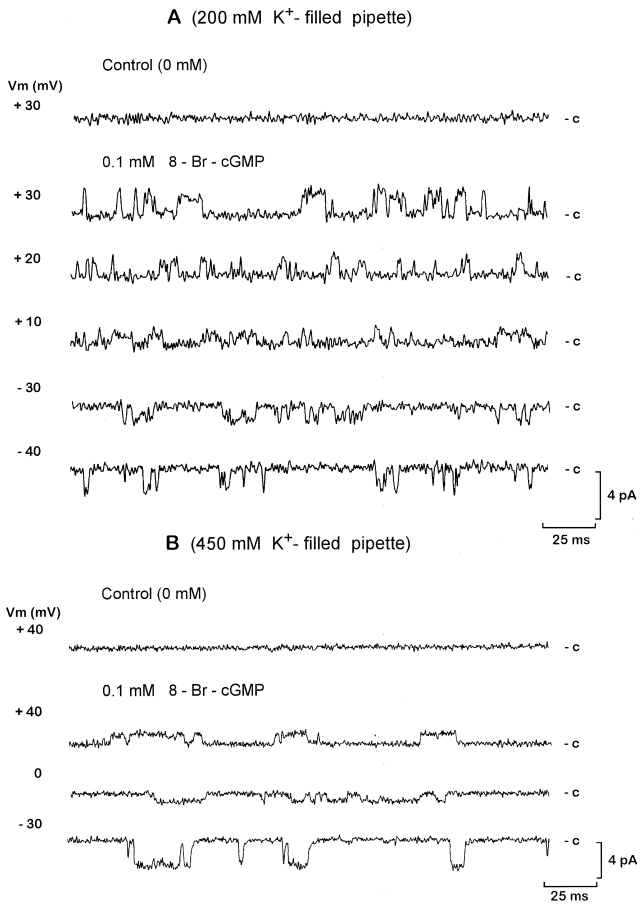

FIGURE 10. Effects of membrane potential on the cGMP-activated channel currents, using 200-mM (A) and 450-mM (B) K^+-filled pipettes. Records in A and B were obtained from different Ip-2 cells. The channels were activated by application of 0.1 mM 8-Br-cGMP while Vm was held at each of the indicated values. Closed channel states (baselines) are shown on the right of each trace (-c). In A, it was computed that P_O increased with depolarization: P_O = 12% at Vm = 30, 9.0% at 20, 4.0% at −30, 1.0% at −40 mV.

−30 and for those at Vm of 20 mV are shown in Table II.

In Fig. 9 B, the histograms could be well fitted by the sum of two exponentials with relative contents of the areas (decimal values in parentheses), the open time constants τ_{o1}, τ_{o2}, and the closed time constants τ_{c1}, τ_{c2}, similar to those of the light-dependent channels before excision. At Vm = −30 mV and 0.2 mM cGMP, the open time constants gave τ_{o1} = 0.22 for the short component and τ_{o2} = 2.7 ms for the long component. The mean open time constant τ_o was computed to be 0.37 ms under this condition. At the same Vm = −30 mV, but at higher 2 mM cGMP, their constants were 0.38 for τ_{o1}, 1.3 for τ_{o2}, and 0.43 ms for τ_o. These open time constants at Vm = −30 mV, and the concerned open time constants at a depolarized Vm = 20 mV are averaged in Table II. As noted above, very small values of τ_{o1} near the time resolution limit (0.16 ms) of the 1 KHz low-pass filter, e.g., 0.22 ms and 0.38 ms, are neither accurate nor reliable and true values may be shorter (see DISCUSSION). In spite of such an inaccuracy, this result suggested that τ_{o1}, τ_{o2}, and τ_o of the cGMP-activated channels are not significantly changed by differences in cGMP concentration of 0.2 and 2 mM and in Vm's of −30 and 20 mV.

On the other hand, at Vm = −30 mV and 0.2 mM cGMP the closed time constants were τ_{c1} = 8.0 for the short component, τ_{c2} = 34 for the long component, and τ_c = 25 ms for the mean closed time, and at the same −30 mV, but at 2 mM cGMP, they were 5.7 for τ_{c1}, 20 for τ_{c2}, and 15 ms for τ_c. The averaged values for these closed time constants at Vm = −30 mV and for those at a depolarized 20 mV are summarized in Table II. This showed that τ_{c2} and τ_c are significantly reduced with increasing cGMP ($P < 0.02$). Thus, these results suggest that P_O of the cGMP-activated channel increases with increasing cGMP concentration and also with depolarization, without significant changes in any of τ_{o1}, τ_{o2}, or τ_o.

Fig. 10 shows examples of the channels in the inside-out patches of Ip-2 cells at different membrane potentials, activated by 8-Br-cGMP. The unitary currents activated by the same 0.1 mM 8-Br-cGMP were recorded while the membranes were held at positive potentials or at negative potentials, using both 200-mM (A) and 450-mM (B) K^+ pipettes. In both A and B the inward currents in the negative Vm decreased as the membrane was depolarized, and reversed sign from inward to outward with a more positive depolarizing shift of Vm, as expected for a K^+-selective channel. In the same manner as shown in Table II, a kinetic analysis showed that $P_o$of the cGMP-activated channels is higher at positive depolarized Vm (Fig. 10 A).

Comparison of Kinetics of the Light-dependent and cGMP-activated Channels

As summarized in Table II, the open and closed time distributions of the cGMP-activated channels were compared with those of the light-dependent channels before excision. In both the channels, the open time constants τ_{o1}, τ_{o2}, and the mean open time τ_o were similar to each other and were also not altered by membrane voltages. As noted above, however, the similarity of very short τ_{o1}s between both the channels would be unreliable, because of the time resolution limits of the 1 KHz low-pass filter and other experimental apparatus. The closed time constants τ_{c1}, τ_{c2}, and τ_c were similar to each other in the both channels, although any τ_{c2}s were significantly shorter in the cGMP-activated channels ($P < 0.02$–0.05). P_Os of both the channels increased with depolarization, and the rise of P_Os did not affect any of τ_{o2} or τ_o in both the channels. Thus, these findings show that the kinetics of the light-dependent channels

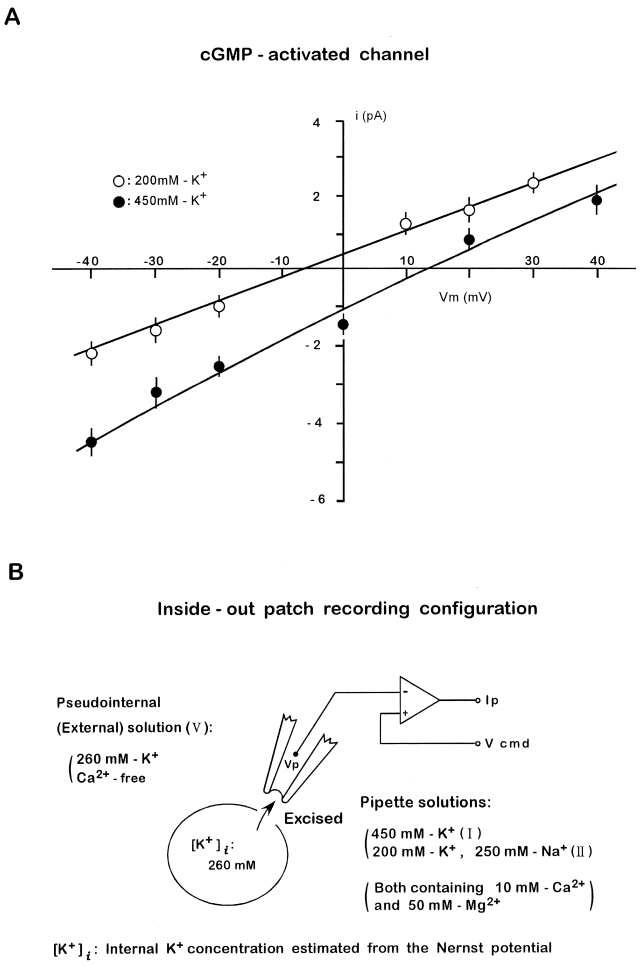

FIGURE 11. (A) i-V relations for the cGMP-activated channel currents, using 200-mM(○) and 450-mM(●) K^+-filled pipettes. The data were obtained from experiments of the same series as shown in Figs. 8 and 10. Each solid line shows the i-V relation curves obtained from the GHK equation (Eq. 2), using the same values of P_K as those estimated for the light-dependent channels and V value of -Vp. These curves were well superimposed by the best-fit curves of the GHK equation (Eq. 2) (not depicted). This indicates that both the cGMP-activated and light-dependent channels have the same conductance. Reversal potentials were, -6.5 ± 0.5 (mean ± SEM, $n = 10$) at 200-mM K^+ and 13.5 ± 0.7 mV (mean ± SEM, $n = 5$) with 450-mM K^+ pipettes, consistent with a K^+-selective channel. Symbols indicate the mean and vertical bars ± SEM of the data points from 5 to 10 excised patches. (B) A sketch map showing experimental conditions underlying the excised patch recording to obtain i-V relations in A.

are similar to those of the cGMP-activated channels after excision, except for a few differences in the channel kinetics (see DISCUSSION).

Ionic Selectivity and Conductance of the cGMP-activated Channel

The single-channel i-V relationships for the cGMP-activated channels obtained from experiments of the same type as those shown in Fig. 10 are plotted in Fig. 11 A. The best-fit GHK curves (solid lines) were drawn in the same way as in Fig. 6. The single-channel current reversed at Vm of -6.5 ± 0.5 mV (mean ± SEM, $n = 10$) with 200-mM K^+ (open circles) and at Vm of 13.5 ± 0.7 mV (mean ± SEM, $n = 5$) with 450 mM K^+ (closed circles) pipettes. The K^+ concentration of the pseudointernal solution (V) was set to the estimated $[K^+]_i$ of 260 mM as shown in Fig. 6 C and Fig. 11 B. Then, if the cGMP-activated channel is K^+ selective, it should reverse at Vm = −6.7 mV with the 200-mM K^+ pipette and at Vm = 14.1 mV with the 450-mM K^+ pipette, which correspond to E_K of the excised membrane predicted by the Nernst equation. Thus, the reversal potentials measured above were very close to these predictions. This indicates that the cGMP-activated channels are primarily selective for K^+, just the same as the light-dependent K^+ channels.

In the previous section (Fig. 6), i-V relations for the light-dependent channels were predicted by the GHK equation (Eq. 2). We tested whether i-V relations for the cGMP-activated channels can also be predicted by this equation. Then, when we take the K^+ permeability (P_K) to be the same as that estimated for the light-dependent channels, and V, i.e., Vm to be −Vp in the excised patch of Vw = 0, the curves of the GHK equation (Eq. 2) fitted well to the data points (Fig. 11 A). This signified that these i-V curves for each channel obtained using 200-mM K^+ and 450-mM K^+ pipettes, are accurately superimposed by the i-V curves for the light-dependent channels. Thus, the K^+ selectivity, permeability and conductance of the cGMP-activated channels are the same as those of the light-dependent channels.

Finally, we conclude that the cGMP-activated channel in Ip-2 or Ip-1 cells is identical with the light-dependent K^+ channel before excision, on the basis of K^+ selectivity, K^+ permeability, conductance, and kinetics. In addition, the light-dependent K^+ channels of Ip-2 opened by light may also be equal to those of A-P-1 closed by light, because both have similar channel characteristics and both are activated by the same cGMP.

DISCUSSION

In the present study, the properties of light-dependent K^+ channels underlying a hyperpolarizing receptor potential in the simple photoreceptor, Ip-2 or Ip-1 cells (Fig. 1 A), were examined by the cell-attached and inside-out patch clamp techniques, and compared with those in the A-P-1 or Es-1 cells depolarized by light. The results show that the hyperpolarizing photoresponse of Ip-2 or Ip-1 is produced by opening of only one class of the light-dependent K^+ channels similar to that of A-P-1.

So far, no detailed identification of light-dependent single-channels has been accomplished on at least in-

vertebrate photoreceptors, because of a shortcoming in former experiments where the cell-attached recordings were conducted without holding their membrane potentials constant. In fact, Bacigalupo et al. (1986) and Johnson et al. (1991) showed that the depolarizing response of *Limulus* ventral photoreceptors results from only one type of light-dependent channel having at least two different conduction states in the same channel. However, on the same *Limulus* ventral photoreceptors Nagy and Stieve (1990), Nagy (1990), and Deckert et al. (1992) reported that there are three types of light-dependent channels which differ in their kinetics and reversal potentials. Furthermore, the above shortcoming without voltage clamping has hindered identifying definitely a second messenger that opens light-dependent channels on the invertebrate ocular photoreceptors. For example, the patch clamp analyses of *Limulus* ventral photoreceptors have shown that the light-dependent channel is activated by a second messenger, cGMP (Bacigalupo et al., 1991). However, in the same *Limulus* photoreceptors, at least the initial part of the depolarizing photoresponse has been reproduced by intracellular injection of IP_3 or Ca^{2+} (Frank and Fein, 1991), and the cell-attached single-channel recordings have shown that two or three classes of light-dependent channels coexist in the same membrane, suggesting multiple second messenger systems (Nagy, 1993).

A marked feature of the present cell-attached patch recording experiments is that photoreceptor cells were held at a constant membrane potential, Vw of −14 mV for Ip-2 or Ip-1 cells (−20 mV for A-P-1 cells), due to replacing normal ASW with modified ASW, regardless of dark or light. This constant voltage of the cell made it possible to determine whether the light-dependent single-channel currents result from a definite conductance state of the same kind of channels during the full course of the macroscopic photoresponse.

The open and closed time distributions of the light-dependent K^+ channels fitted well by the sum of two exponentials with the short and long open time constants τ_{o1} and τ_{o2} and with the short and long closed time constants τ_{c1} and τ_{c2}, respectively, suggesting the existence of at least two open and two closed states.

The reversal potentials of the light-dependent channels, measured with the patch pipettes containing two different K^+ concentrations of 200 and 450 mM, were always nearly equal to E_K of the patch membrane derived from the Nernst equation. These reversal potentials were also not affected by replacing Ca^{2+} or Mg^{2+} in the pipette solutions with sucrose (unpublished data). Our macroscopic experiments have shown that the reversal potentials of the hyperpolarizing photocurrents in external 10 mM (normal) or 20 mM K^+ ASW are almost unaltered by reduction of the $[Na^+]_o$ or the $[Cl^-]_o$ to 20% or 10% of normal due to Na^+ or Cl^- substitution (Nishi and Gotow, 1998). These findings suggest that the light-dependent channel is predominately K^+ selective under physiological ionic conditions such as K^+, Na^+, Ca^{2+}, Mg^{2+} and Cl^-, i.e., contributions of these ions except for K^+ to this channel are negligible.

Comparison of Light-dependent K^+ Channels with cGMP-activated Channels in the Same Patch Membrane

To test the question of whether cGMP activates the light-dependent K^+ channel, we applied cGMP to the cytoplasmic sides of the excised inside-out patch. The present results provided direct evidence that the channel opened by light (the light-dependent K^+ channel) in the intact Ip-2 or Ip-1 cells is the same as the channel activated by cGMP (the cGMP-activated channel). It is unlikely to be mediated by phospholylation or other chemical reaction with soluble factors, because this activation in excised patches occurred in the absence of ATP or GTP and other soluble molecules. Thus, the results suggest that the channels were directly activated by cGMP. A precedent for involvement of cGMP activating (opening) a light-dependent K^+channel has been found in a different ocular system, the *Pecten* ciliary hyperpolarizing photoreceptor (Gomez and Nasi, 1995). However, there remains some uncertainty in this study regarding whether the light-dependent K^+ channel in intact cells is identical to the cGMP-activated channel in the excised patch.

The open and closed time distributions of the cGMP-activated channels were also fitted by the sum of two exponentials with short, τ_{o1} and long, τ_{o2} time constants and with short, τ_{c1} and long, τ_{c2} time constants, respectively, similar to those of the light-dependent channels (Table II). However, an open time constant (τ_{o1}) for the short components of channel events introduces a considerable error due to the time resolution limit of a 4-pole low-pass filter at 1 KHz (see MATERIALS AND METHODS) and other experimental devices, such as the patch-clamp amplifier and capacitance of patch-pipettes. The low-pass filter sets an effective limit of $1/(2\pi\ fc) = 0.16$ ms to resolve the time constant of dwell-time distribution. For example, if the real τ_{o1} is equal to 0.16 ms, the obtained (observed) time constant is expected to be ~1.5 times longer (0.24 ms) than the real one after filtering. Thus, the real τ_{o1}s in Fig. 9 are inaccurate and may be shorter. In other words, τ_{o1}s in Table II containing Fig. 9 would be inaccurate and unreliable. Moreover, these would contain sampling and fitting errors due to missing of short open or closed events shorter than 0.2 ms.

In spite of such an inaccuracy, in both of the channels, τ_{o1} and τ_{o2}, and the mean open time, τ_o were apparently independent of light intensity or concentration of cGMP and membrane potential. In contrast to

open time constants, τ_{c2} and the mean closed time, τ_c obviously decreased in both cases with increasing light intensity or cGMP, although τ_{c1} was relatively unchanged with them. In addition, in both channels, P_O increased with depolarization and its increase in P_O did not affect any of τ_{o2} and τ_o. However, there were a couple of differences between the kinetics of cGMP-activated and light-dependent channels. The relative content of τ_{o2} or the τ_o was a little smaller in the cGMP-activated channels and the τ_{c2} was generally longer in the light-dependent channels. These findings may reflect differences between modes of channel activation: the response to light showed an early phase of high activity and a late phase of declined low activity of the channels, whereas a maintained uniform channel activity was observed during application of cGMP. We cannot answer definitely why these differences occurred, but some reasonable inferences are possible. One is the existence of various cytoplasmic factors which interfere with the open and shut kinetics of the channel, by reversibly binding to the channel molecule or reacting with and modifying it. Another is the difference in cGMP metabolic conditions between the cytoplasm and pseudointernal solution of the inside-out patch. The difference in closed time distribution (τ_{c2}) may be explained by the difference in cGMP concentration. However, it is difficult to determine the metabolic concentration of cGMP that moderately activates channels in the intact cell.

Thus, except for two or more disagreements of the open and closed channel time distributions, we conclude that the cGMP-activated channel is identical to the light-dependent K^+ channel in that both have similar kinetic properties, K^+ selectivities, P_Ks, and channel conductances.

In the *Aplysia* extraocular photoreceptor R2, similar to Ip-2 cell, it has been reported that the hyperpolarizing photoresponse due to an increase in the K^+ conductance is mediated by the Ca^{2+}-activated K^+ conductance, showing that Ca^{2+} acts as an internal transmitter (Brown and Brown, 1973; Brown et al., 1975). However, we have found in the Ip-2 cells that both the light-dependent and cGMP-activated K^+ conductances are completely blocked by 4-aminopyridine (0.1 mM), an extremely powerful blocker of the light-dependent K^+ channel in *Pecten* ciliary photoreceptors (Gomez and Nasi, 1994), although this blocker has been found to have no effect on the Ca^{2+}-activated K^+ conductance (Gotow et al., 1997; Nishi and Gotow, 1998). In contrast, TEA (5 mM), an effective blocker of Ca^{2+}-activated K^+ channel of the *Aplysia* neurons (Herman and Gorman, 1981), abolished the Ca^{2+}-activated K^+ conductance of Ip-2 cells without any effects on both the light-dependent and cGMP-activated K^+ conductances (Nishi and Gotow, 1998). Together with the present results, these findings showed that the light-dependent K^+ conductance in the *Onchidium* simple (extraocular) photoreceptor differs clearly from the Ca^{2+}-activated K^+ conductance, contrary to the *Aplysia* hyperpolarizing photoresponse.

We have provided a precedent in the invertebrate phototransduction that the light-dependent K^+ channel of A-P-1 or Es-1 cells (which is opened by internal cGMP levels during dark) closes when light reduces their cGMP levels, thereby producing a depolarizing photoresponse (Gotow and Nishi, 1991; Gotow et al., 1994), in a similar way to the vertebrate cGMP cascade (for review see Yau and Baylor, 1989). However, the present hyperpolarizing photoresponse was produced by opening the light-dependent K^+ channel. Thus, if cGMP opens this light-dependent K^+ channel, light to Ip-2 or Ip-1 cells must increase the internal cGMP levels. In fact, a previous study has suggested that the hyperpolarization corresponds to an increase in cGMP levels, which results from light-activation of GC, but not from the inactivation of PDE (Nishi and Gotow, 1998). Recently, it has been suggested that in the *Pecten* hyperpolarizing photoreceptors, light activates GC through G-protein (Go) to induce a rise in cGMP and the consequent opening of the light-dependent K^+channels (Kojima et al., 1997; Gomez and Nasi, 2000).

On the other hand, Xiong et al. (1998) have reported that in the parietal eye of the lizard, light inhibits PDE to elevate cGMP levels, thereby leading to the opening of the light-dependent channels and the depolarization.

Finally, we concluded that in Ip-2 or Ip-1 cells, the light-dependent K^+ channel is opened by cGMP, an internal messenger that is increased by light, thereby leading to the hyperpolarizing receptor potential. Together with the A-P-1 cells, the *Onchidium* simple photoreceptors may represent primitive and ancestral forms of vertebrate and invertebrate ocular photoreceptors, which have specialized structures such as microvilli and/or cilia.

We thank Dr. Hiromasa Kijima, Professor emeritus of Nagoya University for carefully reading and helpful suggestions.

Submitted: 6 May 2002
Revised: 22 July 2002
Accepted: 12 August 2002

REFERENCES

Bacigalupo, J., and J.E. Lisman. 1983. Single-channel currents activated by light in *Limulus* ventral photoreceptors. *Nature.* 304: 268–270.

Bacigalupo, J., K. Chinn, and J.E. Lisman. 1986. Ion channels activated by light in *Limulus* ventral photoreceptors. *J. Gen. Physiol.* 87:73–89.

Bacigalupo, J., E.C. Johnson, C. Vergara, and J.E. Lisman. 1991. Light-dependent channels from excised patches of *Limulus* ventral photoreceptors are opened by cGMP. *Proc. Natl. Acad. Sci.*

USA. 88:7938–7942.

Brown, A.M., and H.M. Brown. 1973. Light response of a giant *Aplysia* neuron. *J. Gen. Physiol.* 62:239–254.

Brown, A.M., P.S. Baur, and F.H. Tuley. 1975. Phototransduction in *Aplysia* neurons: calcium release from pigmented granules is essential. *Science.* 188:157–160.

Deckert, A., K. Nagy, C.S. Helrich, and H. Stieve. 1992. Three components in the light-induced current of the *Limulus* ventral photoreceptor. *J. Physiol.* 453:69–96.

Fesenko, E.E., S.S. Kolesnikov, and A.L. Lyubarsky. 1985. Induction by cyclic GMP of cationic conductance in plasma membrane of retinal rod outer segment. *Nature.* 313:310–313.

Finn, J.T., E.C. Solessio, and K.-W. Yau. 1997. A cGMP-gated cation channel in depolarizing photoreceptors of the lizard parietal eye. *Nature.* 385:815–819.

Frank, T.M., and A. Fein. 1991. The role of the inositol phosphate cascade in visual excitation of invertebrate microvillar photoreceptors. *J. Gen. Physiol.* 97:697–723.

Gomez, M., and E. Nasi. 1994. The light-sensitive conductance of hyperpolarizing invertebrate photoreceptors: a patch-clamp study. *J. Gen. Physiol.* 103:939–956.

Gomez, M., and E. Nasi. 1995. Activation of light-dependent K^+ channels in ciliary invertebrate photoreceptors involves cGMP but not the IP_3/Ca^{2+} cascade. *Neuron.* 15:607–618.

Gomez, M., and E. Nasi. 2000. Light transduction in invertebrate hyperpolarizing photoreceptors: possible involvement of a Go-regulated guanylate cyclase. *J. Neurosci.* 20:5254–5263.

Gotow, T., and S. Hashimura. 1981. Spontaneous activity and action potential of an identified *Onchidium* pacemaker neuron. *Comp. Biochem. Physiol.* 69A:745–757.

Gotow, T. 1989. Photoresponses of an extraocular photoreceptor associated with a decrease in membrane conductance in an opisthobranch mollusc. *Brain Res.* 479:120–129.

Gotow, T., and T. Nishi. 1991. Roles of cyclic GMP and inositol trisphosphate in phototransduction of the molluscan extraocular photoreceptor. *Brain Res.* 557:121–128.

Gotow, T., T. Nishi, and H. Kijima. 1994. Single K^+ channels closed by light and opened by cyclic GMP in molluscan extra-ocular photoreceptor cells. *Brain Res.* 662:268–272.

Gotow, T., T. Nishi, and M. Murakami. 1997. 4-aminopyridine and *l-cis*-diltiazem block the cGMP-activated K^+ channels closed by light in the molluscan extra-ocular photoreceptors. *Brain Res.* 745:303–308.

Hamill, O.P., A. Marty, E. Neher, B. Sakmann, and F.J. Sigworth. 1981. Improved patch-clamp techniques for high-resolution current recording from cells and cell-free membrane patches. *Pflugers Arch.* 391:85–100.

Herman, A., and A.L. Gorman. 1981. Effects of tetraethylammonium on potassium currents in a molluscan neurons. *J. Gen. Physiol.* 78:87–110.

Hodgkin, A.L., and B. Katz. 1949. The effect of sodium ions on electrical activity of the giant axon of the squid. *J. Physiol.* 108:37–77.

Johnson, E.C., J. Bacigalupo, C. Vergara, and J.E. Lisman. 1991. Multiple conductance states of the light-activated channel of *Limulus* ventral photoreceptors. Alteration of conductance state during light. *J. Gen. Physiol.* 97:1187–1205.

Kojima, D., A. Terakita, T. Ishikawa, Y. Tsukahara, A. Maeda, and Y. Shichida. 1997. A novel Go-mediated phototransduction cascade in scallop visual cells. *J. Biol. Chem.* 272:22979–22982.

Matthews, G., and S.-I. Watanabe. 1987. Properties of ion channels closed by light and opened by guanosine 3′,5′-cyclic monophosphate in toad retinal rods. *J. Physiol.* 389:691–715.

Nagy, K. 1990. Kinetic properties of single-ion channels activated by light in *Limulus* ventral nerve photoreceptors. *Eur. Biophys. J.* 19: 47–54.

Nagy, K., and H. Stieve. 1990. Light-activated single channel currents in *Limulus* ventral nerve photoreceptors. *Eur. Biophys. J.* 18: 221–224.

Nagy, K. 1993. Cyclic nucleotides and inositol trisphosphate activate different components of the receptor current in *Limulus* ventral nerve photoreceptors. *Neurosci. Lett.* 152:1–4.

Nasi, E., and M. Gomez. 1992. Light-activated ion channels in solitary photoreceptors of the scallop *Pecten irradians*. *J. Gen. Physiol.* 99:747–769.

Nishi, T., and T. Gotow. 1989. A light-induced decrease of cyclic GMP is involved in the photoresponse of molluscan extraocular photoreceptors. *Brain Res.* 485:185–188.

Nishi, T., and T. Gotow. 1992. A neural mechanism for processing colour information in molluscan extra-ocular photoreceptors. *J. Exp. Biol.* 168:77–91.

Nishi, T., and T. Gotow. 1998. Light-increased cGMP and K^+ conductance in the hyperpolarizing receptor potential of *Onchidium* extra-ocular photoreceptors. *Brain Res.* 809:325–336.

Solessio, E., and G.A. Engbretson. 1993. Antagonistic chromatic mechanisms in photoreceptors of the parietal eye of lizards. *Nature.* 364:442–445.

Xiong, W.H., E.C. Solessio, and K.-W. Yau. 1998. An unusual cGMP pathway underlying depolarizing light response of the vertebrate parietal-eye photoreceptor. *Nat. Neurosci.* 1:359–365.

Yau, K.-W., and D.A. Baylor. 1989. Cyclic GMP-activated conductance of retinal photoreceptor cells. *Annu. Rev. Neurosci.* 12:289–327.